Biosystems Engineering, Volume 207, July 2021, pp. 92-105
DOI: 10.1016/j.biosystemseng.2021.05.001

Investigation of the potential to reduce grain waste through sampling and spatial analysis of grain bulks

R. Kerry[1], B. Ingram[2], E. Garcia-Cela[3], N. Magan[4]
[1]*Department of Geography, Brigham Young University, Provo, UT, USA.*
[2]*Facultad de Ingeniería, Universidad de Talca, Chile.*
[3]*Clinical, Pharmaceutical and Biological Science, University of Hertfordshire, Hatfield. 9 AL10 9AB, UK*
[4]*Applied Mycology Group, Cranfield University, Cranfield. MK43 0AL, UK.*

ruth_kerry@byu.edu

Abstract

Batches of grain are accepted or rejected based on the average mycotoxin concentrations from a composite grain sample. Spatial analysis of mycotoxins in two grain bulks was performed to determine the spatial distribution of toxins, whether they were collocated and the proportions of grain over legislative limits. The 2D distribution of deoxynivalenol (DON) and ochratoxin A (OTA) in a truck load of wheat grain was analysed, as was the distribution of fumonisins (FB1 and FB2) in a maize grain pile in 3D. The data had been previously analysed, but results here showed that highly skewed data need to be transformed to properly investigate spatial autocorrelation. In the truck of grain, DON and OTA showed co-variation and OTA, in contrast to previous studies, showed spatial structure when converted to normal scores. Spatial analysis of the maize showed that FB1 and FB2 contamination levels were both highest near the outer face and base of the grain pile. Simulations for both grain bulks showed that for average toxin concentrations close to the legislative limits, the proportions of grain over the legislative limit can vary greatly and be very small when toxin contamination is highly positively skewed. The implications of the results for management were considered. Post-harvest, strategically placed sensors could be used to monitor environmental conditions within the stored grain in real time and detect the first signs of spoilage allowing swift remediative action so less grain is wasted. Pre-harvest approaches for mycotoxin management are suggested as additional food waste reduction strategies.

Keywords: Mycotoxins, grain storage, spatial analysis, variograms, local Moran's I, sequential Gaussian simulation

Introduction

The FAO (2017) estimates the world will need to produce 56% more food to feed over 9 billion world population by the year 2050 (Ranganathan et al. 2018). Searchinger et al. (2019) noted that the key to producing a "sustainable food future," are reducing waste, increasing food production while maintaining (or reducing) the land used in agriculture, and cutting greenhouse gas (GHG) emissions. The pursuits of precision and digital agriculture have the potential for addressing the problems associated with feeding the future global population

whilst not extending the cultivated area and reducing waste could contribute to reductions in GHGs.

Mycotoxins are naturally occurring toxic secondary metabolites produced by fungi in a range of commodities both in the field before harvest and post-harvest during storage (Kushiro, 2008; Wang et al., 2016). Food standard regulations around the world cover a range of mycotoxins which are harmful to human and animal health (Omatayo et al. 2019). The maximum permissible concentrations of mycotoxins that are legislated vary by country, toxin and food commodity (Mazumder and Sasmal, 2001). It has been suggested that lack of legislation for aflatoxin, a mycotoxin that is particularly carcinogenic, in some less developed countries can be linked at least in part to between 2-10 times (Henry et al., 1999) and 16–31 times more deaths from liver cancer in some less developed countries (Liu and Wu, 2010)..

This illustrates the great importance of food safety regulation. However, the testing for mycotoxin contamination is expensive (Papadoyannis, 1990) so it does not take account of spatial variability in the distribution of these toxins within batches of grain and other foodstuffs. The standard protocol is to collect numerous samples at regular intervals throughout a batch of grain. These are then mixed together to make one composite sample in which the mycotoxin levels are measured to represent the average concentration of contamination in the whole batch of grain (EU, 2006a; Maestroni and Cannavan, 2011). This approach could potentially result in large quantities of uncontaminated grain being wasted or pockets of highly contaminated grain being missed if the toxin levels are very high in small, localized pockets within the batch of grain.

Due to this sampling approach, little is known about the spatial variation of mycotoxins in storage settings. Spatial studies of mycotoxins have been minimal due to the costs of testing for mycotoxins. For such studies of representative sampling, validated accredited methods are required to ensure the accuracy of the results. This is expensive, and because of the small margins in the grain industry, it is often thus not carried out. Portell et al. (2020) visually investigated the three dimensional (3D) spatial extent of *Fusarium graminearum* colonization of wheat grain at different moisture contents and following inoculation at different positions within clear storage jars. Colonization dynamics and respiration were affected by the inoculation position but dry matter loss and fungal biomass were mainly affected by the moisture content. Biselli et al. (2008) measured deoxynivalenol (DON) and ochratoxin A (OTA) contamination of 100 samples from a truck load of grain. They compared the average concentrations from a bulked sample with the average concentrations of the 100 individual samples. They found that the former was representative of the latter for DON, but not for OTA, which had a far greater coefficient of variation. Using the same data set, Rivas-Casado et al. (2009a) investigated the spatial structure of DON and OTA variation within the truck- load of grain using variograms. They concluded that DON showed spatial structure but that OTA did not. Rivas-Casado et al. (2009b) then used this information to simulate data sets that could be repeatedly sampled to help determine suitable sampling protocols for the future. The dataset generated by Biselli et al. (2008) showed spatial variation in 2 dimensions (2D), but variation within grain bulks needs to be examined in 3D. Rivas-Casado et al. (2010) sampled stored maize in a silo in 3D with the aim of characterising

the spatial structure and determining a suitable grain sampling and bulking strategy. However, they found no spatial structure in the data so the latter was not possible.

The mycotoxin levels in the truck load of wheat grain and the maize pile investigated by Rivas Casado et al (2009a) and (2010), respectively were highly skewed. As variograms are based on variances, they can be sensitive to a few large outliers or asymmetry in the data distribution (Kerry and Oliver 2007a,b). Rivas Casado et al., (2009a, 2010) did not employ any method of dealing with the asymmetry in OTA or FB_1 and FB_2 concentrations, respectively. Typical methods of dealing with asymmetry for variogram computation involve transforming the data to logarithms or indicators, removing outliers or computing normal scores (Kerry and Oliver 2007a,b). The aim of the present study was to re-analyse the data investigated by Rivas Casado et al. (2009a) and Rivas Casado et al. (2010) to determine if dealing with the non-normality in the OTA and FB_1 and FB_2 data could reveal spatial structure in OTA, and any spatial association with DON data and whether there was spatial structure in the FB_1 and FB_2 concentrations in 3D.

These aims were partially fulfilled by Kerry et al. (2019a) in an initial examination of the spatial variation in DON and OTA in the truck load of grain and FB_1 and FB_2 in the stored maize grain. Unlike the previous studies of Rivas Casado et al. (2009a,b) and Rivas Casado et al. (2010). However, they did not interpolate (krige) the data to visualize and investigate the proportions of the two grain bulks that were below the legislative limits to quantify the amount of waste that was occurring. This has been was done in the current paper and geostatistical simulation has also been employed to determine the range and degree of uncertainty in the grain proportions that were above the legislative limits for batches of grain with the same variograms but a mean concentration that was equal to the legislative limit. This was done to determine what range of proportions of uncontaminated grain would be wasted in such situations and to suggest future management strategies that could reduce some or all of this waste.

Materials and Methods

Data collection

The data for this paper come from two previous studies. Data on different mycotoxins were collected from two grain bulks, one in a truck and one in a grain pile. The variations in DON and OTA in the truckload of previously stored wheat were examined in two 2D dimensions. The truckload of wheat with dimensions of 2.5 m×10 m was sampled from above in the horizontal plane at a spacing of 0.5 m producing a grid of 100 points (Biselli et al., 2005, Figure 1a). A five-aperture probe sampler was vertically inserted into the grain at each grid point to take a single incremental sample containing grain from five depths. Each sample was mixed and subsampled before the DON and OTA concentrations were measured. Full details of the lab procedures used are given in Biselli et al. (2005). The final sets of values describe the spatial variation of DON and OTA concentrations (µg kg^{-1}) in a two-dimensional

horizontal plane but as values are averaged with depth, there is no insight into how DON or OTA changed with depth.
Data were collected from the stored maize grain pile in 3D. A bed of maize in a large grain store with an exposed surface area of ~ 3800 m^2 and height of ~10 m was sampled in three planar layers inclined at 45°, parallel to the open face of the bed, providing a three D dimensional grid of points (Rivas Casado et al., 2010, Figure 1b). There were 50 points in each layer on a 10 × 5 point grid with a 0.5 m spacing between points. There was also a spacing of 0.5 m between each of the layers (Figure 1b). Grain samples were taken using probe with a conical chamber at the tip that could be opened and closed using a lever at the end of the shaft (Figure 1c), collecting about 200 g of grain. A 0.5 m square metal frame was placed on the exposed grain face to locate the sampling points where the probe would Samples from the three different layers were taken at each point before moving the frame to minimize disturbance of the grain (Rivas Casado et al., 2010).

The FB_1 and FB_2 contents were analyzed using the validated method detailed in Rivas Casado et al. (2010). Samples were ground, passed through a 1 mm sieve and homogenized. A solution of acetonitrile:methanol:water (25:25:50, v/v/v) was used to extract fumonisins with a grain to solution ratio of 1:5. Following further sample preparation concentrations of FB_1 and FB_2 (μg kg^{-1}) were determined using a liquid chromatography–mass spectrometry system (Thermo-Fisher Scientific, San Jose, CA, USA)

Data analysis

The OTA data from the truck load of grain were transformed to normal scores (NS). Normal score ties were broken using the local mean of the eight nearest neighbor points. Normal scores were calculated in the same way for FB_1 and FB_2 from the grain pile. Omni-directional variograms in two dimensions with a lag separation of 0.5 m were computed and modelled for DON and OTA in the truck load of grain and FB_1 and FB_2 in each layer of the grain pile using SpaceStat (Jacquez et al., 2014). A two-dimensional cross-variogram with a 0.5m lag was computed between DON and OTA NST for the truck load of grain using SGems (Remy et al., 2009). Omni-directional variograms in three dimensions with a lag separation of 0.5m were computed for FB_1 and FB_2 concentrations in the grain pile using SGems (Remy et al., 2009). Residual maximum likelihood (REML) variograms were also computed for FB_1 and FB_2 in each layer of the grain pile using GeoR (Ribeiro *et al.*, 2001).

The global Moran's I statistic investigates the spatial autocorrelation. It involves standardizing data to a mean of zero and unit variance and this can be problematic when data are highly skewed. However, in using the mean and standard deviation of a local neighbourhood to standardize data, the local Moran's I (LMI) is less likely to encounter problems with skewed data. Univariate global and LMI analysis (Anselin, 1995) was done using SpaceStat for DON and OTA NS from the truckload of grain and for the FB_1 and FB_2 concentrations of the individual layers in the grain pile. The global Moran's I statistic determines if there is significant positive (clustering) or negative (spatial outliers) spatial autocorrelation in the data compared to a spatially random distribution. The LMI statistic computes the statistic for a moving window to determine if a given observation is similar or

different to the mean of neighbouring values (here within 1m). Maps were produced to show whether points were part of significant (p=0.05) clusters of low (LL- low values surrounded by low values) or high (HH – high values surrounded by high values) values, were significant spatial outliers (LH – low values surrounded by high values or HL – high values surrounded by low values) or were not significantly (NS) different from a random distribution. Monte Carlo simulation was used to determine the p-value of the LMI statistic for each observation. The number of tests was large and each point is reused in several tests so the risk of false positives was increased hence the Simes correction (Jacquez et al. 2014) for multiple testing was used to adjust for this. Bivariate global and LMI analysis between DON and OTA NS in the truck load of grain and between different layers for FB_1 and FB_2 in the grain pile was performed. This indicates if clusters in the two variables or layers are collocated by using the standardized values of the second variable as the neighbours for each point in the first variable. This means that HH and LL clusters are significant clusters with high or low values, respectively of both variables or in both layers and show positive spatial correlation in the variables. Any HL or LH clusters indicate significant clusters of high values in the first variable and low values in the second variable, or low values in the first and high values in the second variable. Such locations show negative spatial correlation between variables.

The 2D variograms for truck load of grain were used to ordinary krige the raw DON and OTA NS data to a 0.1 m grid to give a more complete picture of likely variation of DON and OTA in the grain. Kriged OTA NS data were back-transformed to the original scale following kriging. This analysis was performed in SpaceStat (Jacquez et al., 2014). The 3D variograms for the FB_1, FB_2 NS data in the grain pile were used to ordinary krige the values to a 0.05 m grid. Following kriging, 3D local Moran's analysis of FB_1 and FB_2 was performed following the approach of Kerry et al. (2017) and kriged NS values were back-transformed to the original scale.

Finally, the mycotoxin data for the truck of wheat grain and the maize grain pile and their associated histograms and variograms were used for conditional sequential Gaussian simulation (SGS) of the data to 0.1 m and 0.05 m grids, respectively in SGems (Remy et al., 2009). SGS converts data to NS so that data being simulated have a normal distribution. Following simulation, the values are back-transformed to the original scale. Here 100 realizations were simulated for each dataset. The simulated values were converted to z-scores (zero mean and unit variance) by subtracting the mean from each value and then dividing by the standard deviation of the original dataset. Although data for OTA and FB_1 and FB_2 were highly positively skewed, the values of the z-scores reflected this with fewer negative z-scores and more positive and large z-scores. These z-scores from simulation were analyzed to compute summary statistics for the 100 realizations and determine what proportion of points were above the mean of zero and would be rejected in a scenario where the mean concentration was equal to a legislative limit.

Results and Discussion

Frequency Distribution of Mycotoxins

Figure 2 shows the histograms for DON and OTA contamination in the truck load of wheat. DON had a relatively normal distribution with a slightly elevated skew (1.21) caused by a large outlier and slight asymmetry (Figure 2a). DON had a large range of values of up to ~2700 µg kg^{-1} and there were no points with 0 ppb. Most points had values between 1000 and 1500 µg kg^{-1}. The histogram for OTA (Figure 2b) showed a highly skewed (4.36) distribution, approximating a Poisson distribution, with a large number of points with 0 ppb and the highest concentration being ~9 ppb. Most values in the distribution are below 1 µg kg^{-1}. Rivas-Casado et al (2009a) noted the strongly skewed distribution of the OTA data but did not address this problem although they log- transformed the DON data, which were far less skewed. The histograms in Figure 3a, b show the distribution of FB_1 and FB_2 in the stored maize grain pile. Both histograms showed marked asymmetry and FB_2 had a larger skew (1.91). For FB_1, the values reached up to ~8000 µg kg^{-1} whereas maximum values for FB_2 were ~6000 µg kg^{-1}. For FB_1, most of the values were below 4000 ppb whereas for FB_2, most values were below 2000 µg kg^{-1}. The positively skewed distributions of all of the toxins examined in the truck and the grain pile suggests that concentrations of mycotoxins typically have skewed concentrations. Indeed, it is well known that environmental contaminants often have highly skewed distributions (Goovaerts et al. 1997; Van Meirvenne and Goovaerts, 2001) and this has implications for how the pollutant is dealt with or managed.

Spatial Analysis

Variogram and Moran's I Analysis of DON and OTA Contamination in a Truck load of Grain

As the histograms for each mycotoxin showed marked asymmetry the use of log transformed and normal score transformed data (Webster and Oliver, 2007) was investigated for computing variograms and the Moran's I. Table 1 shows the variogram parameters for DON and OTA contamination in the truck load of grain. The raw DON values showed good spatial structure with a variogram range of 4 m and nugget:sill ratio of about 13% (Figure 2c). These parameters were similar to those found for the log-transformed data by Rivas-Casado et al. (2009a). The variogram for OTA (Figure 2d) had a similar range to that of DON but a large nugget effect (62 %, Table 1) showing a large proportion of spatially random variation. However, the variogram of OTA NS (Figure 2e) had a nugget:sill ratio of 30% and the range decreased to 1m suggesting that patches with similar values were small. However, these smaller patches could appear as a greater proportion of random variation if the skewed data were not dealt with. Rivas Casado et al. (2009) suggested that there was no spatial structure in OTA perhaps due to the high proportion of nugget variation, but after dealing with the highly skewed data using NS new patterns were found. The global Moran's I values (Table 1) also agree with these findings. Raw DON values showed strong (0.468) positive and significant (p=0.001) spatial autocorrelation. In contrast raw OTA values showed negative spatial autocorrelation that was not significant (p=0.494) whereas the OTA NS data showed moderate, positive and significant spatial clustering (p=0.001). These results show that highly skewed data need to be transformed to properly investigate spatial autocorrelation in their patterns.

Figure 4a and c show the spatial patterns of the raw values of DON and OTA in the truck. These patterns show most spatial variation occurring along the long axis of the truck which

is consistent with the method of loading the truck. Indeed, examination of directional variograms (not shown) for the long and short axis of the truck showed spatial structure for the long axis with parameters almost identical to the omni-directional variogram and predominantly random variation across the short axis of the truck. Rivas-Casado et al. (2009a) also observed similar differential spatial variation in the long and short axis of the truck. However, they concluded that the seemingly random variation across the short axis was a result of it being so short and there being low numbers of comparisons at each lag. Figure 4b and d show how DON and OTA values are clustered in space using the univariate local Moran's I. These maps are consistent with the findings of the variogram and global Moran's I analysis in that they show larger significant clusters of HH and LL points for DON than for OTA.

The last row in Table 1 reports the parameters of a cross-variogram between DON and OTA NS (Figure 2f). This showed spatial structure and co-variation in the two toxins with patches of similar values with a diameter of ~3m. The bivariate LM (Table 1) also showed significant (p=0.001) spatial association between DON and OTA NS as did the bivariate local Moran's I (Figure 4e). The bivariate LMI results (Figure 4e) showed areas with significant values exhibiting both positive (HH and LL, red and dark blue) and negative spatial (HL and LH, pink and pale blue) association between DON and OTA. Thus, correlation between the two toxins is missed by standard correlation coefficients (Spearman's r<0.1, p>0.05) as the correlation changes from positive to negative locally. Figure 5a and b shows the kriged DON and OTA NS respectively. The patterns of variation in kriged DON and OTA NS are smoother and more continuous than for the raw data. This translates into a larger patch of LL values in the univariate LMI for DON and larger LL and HH patches in the OTA NS univariate LMI than for the raw data. This also further emphasizes that there are places in the truck load of grain where DON and OTA values are both positively (red and dark blue) and negatively (pink and pale blue) associated (Figure 5e).

The spatial analyses suggest that clusters of DON and OTA are often co-located, but the patches of OTA are smaller. As DON is usually produced in the field (Kushiro, 2008) and OTA during storage (Wang et al., 2016). This finding is consistent with OTA developing from locations of high DON concentrations and spreading out from them. Although the two toxins are produced by different species of fungi, Hussein and Brasel (2001) noted that more than one toxin may show high concentrations in the same initiation points because mycotoxins weaken the host, which improves the environment for further fungal development. The patterns observed are also consistent with the notion that in storage settings, pockets of increased moisture may favour fungal development and toxin production by more than one fungal species. Fungal development is not possible under 0.70 water activity (a_w) equivalent to about around 14-15% moisture content (MC) in wheat and maize. However, small increases in humidity can allow the growth of xerotolerant/xerophilic fungi such as *Penicillium verrucosum* (responsible for OTA contamination). Storage of cereals in silos represent a complex ecosystem, the metabolic activity and damage due to insect pests or of these primary species can result in an increase in moisture content in small pockets, facilitating initiation and colonisation by such mycotoxigenic spoilage fungi. Indeed, numerous studies showed increased fungal growth of a range of species when moisture

availability and temperature become conducive for spore germination and colonisation (Garcia-Cela et al., 2018; 2019; Magan et al., 2020).

Variogram and Moran's I Analysis of FB_1 and FB_2 Contamination in the Grain Pile

Variograms in 3D of raw and log-transformed data were erratic or pure nugget. This is consistent with the findings of Rivas-Cosado et al. (2010). but 3D variograms for NS FB_1 and FB_2 contamination in the maize grain showed spatial structure with areas of similar values of 4 and 3 m diameter, respectively. Both toxins also showed ~ 50% spatially random variation (Table 2 and Figure 3c). The effect of skew on data can be more pronounced when datasets are small, so it is not surprising that the MoM variograms for the individual layers were predominantly erratic or pure nugget. Nevertheless, the REML variograms for layer 1 (FB_1 and FB_2) and layer 2 (FB_1) showed some spatial structure as did the MoM variograms for layer 3 (FB_1 and FB_2) (Table 2). These variograms showed a decreasing range with depth of layer from the exposed grain face (see Figure 1a). For FB_2 a similar pattern to FB_1 was apparent but there was no spatial structure in layer 2 and the patches of FB_2 were smaller than those of FB_1 in both layers 1 and 3. This means that larger patches of both toxins were found in the outer layers of the stored grain and smaller patches or random variation were found closer to the wall of the silo (Figure 1a). This could be a function of the degree of aeration and moisture in the outer and deeper layers of the grain pile, as fungi are aerobic microorganisms that need oxygen (Semple et al., 1989). However, the spatial variation in fungal development and environmental conditions needs further testing.

Global Moran's I (Table 2) and variogram analysis showed that there was a lot of spatially random variation and when there was spatial structure, it was closest to significant in layers 1 and 3. Although the *p* values for none of the layers were significant (p=0.05). The bivariate Moran's I values between layers showed that there was more spatial association between layers 2 and 3 for both toxins and this was significant at: p=0.003 and p=0.016 for FB_1 and FB_2, respectively. Correlations between FB_1 and FB_2 for each layer and all layers together were strong r>0.9. Figure 6a and b show the front and back view of kriged FB_1 NS values. These show larger values near the base of the grain pile and these larger values extend higher on the front exposed grain face than for layer 3 that is closer to the wall. Figure 6c and d further emphasize these spatial patterns. They showed that 3D LMI maps had HH clusters located near rows 4 and 5 of layers 1 and 2 (Figure 1a) and LL clusters were located in rows 1 and 2 of layers 1-3. The maps of the spatial distribution of high and low values for FB_1 and FB_2 were very similar so the latter are not shown. The spatial analysis showed that FB_1 and FB_2 behave and are located similarly but FB_2 had a shorter variogram range indicating slightly smaller patches of contaminations than for FB_1. Logic might suggest that the distribution of HH and LL 506 clusters within the stored grain reflects a case where moisture gathers under the influence of gravity towards the base of the stored grain and that toxins develop most in the outer layers at the base of the grain pile where oxygen and moisture and moisture supply are greatest. However, this could also be the result of differences in temperature within the grain. The environmental conditions of the grain where toxin levels are highest would need to be measured and monitored to confirm whether this is the case or not. Spatial analysis of mycotoxins and environmental conditions in more stored grain silos

are needed to determine whether the outer layers at the base of grain piles tend to have higher toxin concentrations and if so, why. If these areas are typically at higher risk of contamination then they should be monitored with temperature, moisture and CO_2 sensors. This type of data could be utilised by grain silo managers to help evaluate the temporal relative risk of mycotoxin contamination and take immediate and appropriate remedial action. Garcia-Cela et al. (2020) defined three different risk levels based on the CO_2 production levels in wheat naturally or artificially inoculated with *Fusarium graminearum.* If the level of risk is increased (by increased CO_2) the immediate recommendation is to aerate the silo and reduce the m.c. and thus the colonisation by pockets of mycotoxigenic moulds. If the risk is increased then batches may need to be diverted to animal feed or biogas production.

Estimated Percentages of Grain Discarded and Their Uncertainty

To determine the percentages of each batch of grain that was above the legislated limits, ordinary kriging was used. This interpolated values of each mycotoxin in the truck load of wheat grain and in the maize grain between sampling points. To determine the uncertainty associated with kriged estimates, conditional simulations using the histograms and variograms for each toxin were performed. The SGS data were converted to z-scores with zero mean and unit variance following simulation. This means that a value greater than zero (the mean) would be above the legislative limits and any value less than zero would be below the limit.

Tables 3 and 4 show the percentages of grain that had concentrations greater than the legislative limits for the raw data values and kriged data, respectively. For DON contamination of the truck load of wheat grains, the mean batch concentrations for the raw and kriged data (1342, 1354 µg kg^{-1}) were greater than the EU (2006b) and FDA (2010) limits of 1250 and 1000 µg kg^{-1}, respectively. This means that in both locations, the whole truck of grain would be discarded or would have to be re-purposed for animal feed use rather than for human food use. The FDA (2010) limits for DON used for specific animals, e.g., swine, are as high as 5000 µg kg^{-1}. Re-purposing of the grain for animal feed would of course result in reduced income for these batches of grain. Given that the mean batch concentration was close to the EU limit, only 55% (53% for kriged data) of the grain had concentrations greater than the EU limit. This would mean that almost half the batch of grain, that had concentrations below the EU limit, would be wastefully discarded or re-purposed for a use that would results in a lower price for the farmer. Tables 3 and 4 show that the batch of grain would not be discarded due specifically to OTA contamination as the mean concentrations of 0.57 µg kg^{-1} (and 2.68 µg kg^{-1} for kriged data) are well below the 5 µg kg^{-1} EU (2006b) legislative limit.

The SGS results (Table 5) were used to investigate the uncertainty associated with estimates of the proportion of grain that would be wasted due to DON contamination when the mean DON concentration was equal to the legislative limit. The mean percentage of grain with DON levels above the mean was 53 % with a large range from 9-88 % and an interquartile range of 37-73 %. This suggests that on occasion, data with similar characteristics to this could be produced by grain that only showed 9 % was contaminated at levels above the

legislative limits. However, it may be but equally likely that 88% of the grain had toxin levels above the legislative limits. This suggests a quite a wide range of uncertainty in the proportions of values that are above the legislative limits. However, DON concentration in the truck, showed spatially structured variation and little random variation (Figure 2f and Table 1). and a distribution that was not too strongly skewed (Figure 2a). Therefore, if the average DON concentration was at the legislative limit, on average one can expect slightly over half of the grain to be contaminated above legislative limits. For OTA, when the mean concentration was at the legislative limits, the mean proportion of grain with concentrations above the legislative limits was 26 % with a range of 13-36 % and interquartile range of 22-29 %. This means that given data with such a high level of skewness, the mean 581 concentration could be at the legislative limit but on average only 26 % of the grain would have concentrations above the legislative limits. This would result in a significant proportion of wasted grains. There was also less uncertainty in the amount of grain with toxin concentrations above the limits as the range was narrower (13-36%) than for DON (9-88%).

The EU (2006b) has legislative limits of 4000 µg kg^{-1} for the sum of FB_1 and FB_2 in unprocessed maize and 1000 µg kg^{-1} in maize products intended for direct human consumption and the USA has a limit of 4000 µg kg^{-1} for total Fumonisins (FB_1, FB_2 and FB_3) in whole or partially degermed dry milled corn products for human consumption (FDA, 2001). For FB_1 and FB_2 contamination in the maize grain pile, the mean concentration of 3720 µg kg^{-1} (3004 µg kg^{-1} for kriged data) was above the EU (2006b) limit of 1000 µg kg^{-1} limit but below the EU (2006b) and FDA (2001) limits of 4000 µg kg^{-1}. Therefore, the whole batch of maize would be rejected at the 1000 µg kg^{-1} limit but the whole batch would be accepted at the 4000 µg kg^{-1} limit. The distribution of the data was very skewed with many low values and a few very high values (Figure 3 a and b). This is probably responsible for the fact that although only 38% (16 % for 598 kriged data) of the grain had concentrations higher than the legislative limit, the mean concentration of the batch, 3720 µg kg^{-1} (3004 µg kg^{-1} for kriged data), was close to the 4000 µg kg^{-1} limit. In each case, the kriged data showed a smaller proportion of points that were above the over legislative limits than the raw data values. as Kriging has a smoothing effect on spatial distributions. This is fine when trying to get an accurate view of the over-all distribution, but if the interest is in identifying highly contaminated points that are distributional and spatial outliers, the kriging process tends to smooth and mask this aspect of variation. Nevertheless, the LMI maps for both grain 607 bulks (see Figures 4-6) and the global Moran's I values (see Tables 1 and 2) show that there were very few points that were significant spatial outliers and that clustering of high and low values dominated the grain bulks.

Table 5 shows the summary of the simulated values, for FB_1 and FB_2. When the mean concentration of the grain is at the legislative limits, the mean percentages of grain above the legislative limits for the 100 realizations were 43% and 51% for FB_1 and FB_2, respectively. The range of values was 38-48% for FB_1 and 27-72% for FB_2 and the inter-quartile range was 42-44 % for FB_1 and 44-57% for FB_2. These values indicate that for both FB_1 and FB_2, when the mean toxin concentration in the grain is at the legislative limit, on average there was about 50% or less of the grain that had toxin concentrations above the legislative limits. The range of values indicates that there is more uncertainty in the amount of FB_2 than FB_1

locations that were higher than the legislative limits, probably due to the more highly skewed distribution of the data (Figure 3a and b).

Mycotoxins, like any contaminant pollutant in the environment (Goovaerts et al. 1997; Van Meirvenne and Goovaerts, 2001) can have a tendency towards a skewed distribution with a normal distribution contaminated by outliers or lots of low values and a few very high values forming a long positive tail in the distribution. Spatial analysis of the data in general suggest that the distribution of the data should not be ignored when investigating spatial patterns. Also, the simulation analysis suggests that the more skew in the data, makes it likely that a limited number of locations with very high toxin concentrations could cause the average toxin level of a batch of grain to be above the over legislative limits while more than half of the grain had concentrations well below the limits. For DON and FB_1 which showed lower amounts of skew, the amount of grain exceeding legislative limits was around 50% when the mean concentration was equal to the limit, but for the OTA data which were very skewed only about a quarter of the grain exceeded limits when the mean concentration was at the legislative limit and for FB_2, as little as 27% of the grain was contaminated at levels that exceeded the legislative limits.

Spatial identification of the potential contaminant "hot spots" is vital information to prevent and mitigate the mycotoxin accumulation in cereals, and reduces food waste. Since mycotoxins variability in grain bulks is not well understood, the true mycotoxin concentration in a bulk lot cannot be determined with 100% of certainty. Consequently, this can result in contaminated batches being processed while uncontaminated batches can be rejected. As an example, European Legislation requires sampling of 1 kg of cereals by taking 100 incremental samples for cereal lots $\geq$ 50 tonnes (EU, 401/2006a). Understanding the mycotoxin spatial variability could guide the design of accurate and less expensive sampling plans to identify accurately the mycotoxin contamination of each batch. Correct quantification of mycotoxin contamination would reduce human exposure to mis-classified batches. It also allows for bespoke remediation actions to be applied to specific lots for food or feed or could result in highly contaminated batches being diverted for biogas production.

Strategies such as aeration (Akdogan et al., 2006), drying (Magan et al., 2020) or separating the grain at harvest, based on contamination risk into micro batches (Lamb, 2020) could be applied. The variograms for OTA, FB_1 and FB_2 all had considerable nugget components that suggests that there is unresolved spatial variation when sampling at an interval of 0.5m and sampling at a smaller interval could resolve some of this (Webster and Oliver, 2007) and reduce uncertainty from the spatially random component of variation. However, physical sampling destabilizes the grain bulk, making it difficult to conduct denser spatial analysis using traditional sampling methods. A potentially more useful approach that could be employed to reduce uncertainty about the spatial distribution of mycotoxins is to use sensors that provide data on environmental variables such as temperature, CO_2 and relative humidity in different regions of the grain bulk so that a detailed spatial map can be obtained more effectively, and links to detailed mycotoxin contamination levels could be developed on this basis.

Implications of this work

As some co-location of patches of DON and OTA contamination was observed and the former develops in the field and the latter in storage, grain could easily be separated at harvest based on moisture content. Yield monitors, one of the most used precision agriculture 684 technologies, have integrated moisture sensors which measure grain moisture via electrical capacitance (Chung et al. 2016). The moisture sensors are used to correct the measured wet rate of grain flow to dry yield (Reyns et al. 2002). Grain could then be separated at harvest and the wetter grain dried to discourage further fungal development and potential toxin contamination by the same or other fungal species.

The co-location of DON and OTA, show that toxin levels in stored grain can be linked back to environmental conditions and management practices that the crop experienced in the field, as well as how the grain is dried and stored. Numerous studies exist in the precision agriculture literature documenting the identification of fungal infections within fields and the practice of targeted fungicide applications (De Castro et al. 2015a,b, Di Marco et al. 2011; Fischer 2002; Isakeit et al., 2009). As a logical extension of such studies, Kerry et al. (2019b) investigated the spatial variation of aflatoxin levels within two corn (maize) fields in Alabama, USA and were able to establish management zones with different contamination risk. Such zones could be differentially managed by (1) pre-season differential planting rates, planting resistant varieties, (2) within season by differential irrigation and fungicide application rates and (3) at harvest by separating grain with different risks of contamination into micro-batches for storage. Although farmers strive to control fungal infection in the field, the risk of DON contamination pre-harvest for example is based on weather conditions which are uniform within fields. Also, mycotoxin levels are usually only measured at harvest and often ignored in subsequent post-harvest storage settings. Several studies have used hyperspectral imagingery to identify various fungal infections in the field (Mahlein et al. 2012, Del Fiore, 2010). If *Fusarium graminearum* infections that cause DON contamination could be identified in the field using this approachhyperspectral imagery, fungicides could be applied to only the identified infected areas. Another possibility is that fertilizer applications could be reduced in areas with fungal infection. Paungfoo Lonhienne et al. (2015) showed that larger nitrogen fertilizer concentrations can alter the composition of the soil fungal community in favour of species with more pathogenic traits. Limiting or reducing the amount of DON in the field in these ways could potentially result in less OTA development in storage.

The spatial analysis in 3D of the grain pile suggests the need for a post-harvest strategy to reduce waste. Such an approach could also to install a network of Moisture and CO2 and relative humidity sensors throughout stored grain silos to detect initiation spoilage, allowing effective aeration regimes to be instituted or subsequent separation of batches from such a silo that should be discarded and used for biogas production or undergo remedial drying. Currently, such sensors are quite expensive to install. However, with technological developments and the increased use of digital platforms, the economics of such approaches could improve. This would allow effective sampling systems to be developed for ensuring that a true concentration of different mycotoxins can be quantified in cereals destined for either food or feed use.

Conclusions

Variogram and Moran's I analysis of mycotoxin levels in a truck load of wheat and a large maize bulk showed that adjusting for highly skewed data using the NS transform revealed spatial patterns in the data. In the truck load of grain spatial structure in OTA was identified with smaller clusters than DON but with some co-location between DON and OTA clusters. As DON usually develops in the field and OTA during storage, we hypothesize that OTA may be developing from locations of high DON concentrations where the grain is more susceptible to invasion by other fungi or the environmental conditions in the grain are generally favourable for fungal development. In the maize grain pile, spatial analysis showed larger clusters and stronger spatial autocorrelation in the outer grain layers and clusters of high values at the base and low values at the top of the stored grain pile. We hypothesize that this is consistent with humidity diffusing through the grain over time under the influence of gravity and FB_1 and FB_2 tending to develop in wetter grain with more oxygen rich locations at the base and in the outer layers of the stored grain. Future studies need to investigate the spatial distribution, within grain masses, of environmental variables such as moisture, CO_2 and O_2 concentrations that are likely to co-vary with mycotoxins, using robust integrated sensors.

Kriging and simulation showed that in some cases where average concentrations are above legislative limit that would lead to a whole batch of grain being discarded, often less than 50% of the grain was contaminated at levels above the actual maximum allowable levels. This was particularly the case when the data weare very highly skewed. This suggests that current approaches to sampling stored grain for mycotoxins are resulting in a lot of wasted grain. Simulation results showed that there was a greater degree of uncertainty about the spatial distribution of some mycotoxins than others, and this needs further study. Given the quantification of uncertainty, risk can be assessed and managed by specifying the probability of threshold exceedance, to give more control to decision makers. Several strategies for the management of food products earlier in the agricultural food production chain have been suggested in addition to the best practice storage procedures. We believe that management approaches in the field as well as spatial analysis and monitoring of environmental conditions in grain masses post-harvest have the potential to significantly reduce such agricultural waste streams

Acknowledgements

Thanks go to Biselli et al. (2005) and Rivas-Casados et al. (2010) for collecting the mycotoxin data for the truck and the grain pile. In order to cover the complete scope of this research, some of the information and graphics presented by Kerry et al (2019) in a published European Conference of Precision Agriculture conference proceeding is presented here with the permission of Mike Jacobs of Wageningen Academic Publishers.

References

Akdogan, H., & Casada, M. E. (2006). Climatic humidity effects on controlled summer 790 aeration in the hard red winter wheat belt. Transactions of the ASABE, 49(4), 1077-791 1087.

Anselin, L. 1995. Local Indicators of Spatial Association – LISA, Geographical Analysis, 27, 93-114.

Biselli, S., Bruer, J., Persin, M., Schuh, M. and Syben, M. (2005) Investigation of variability associated with testing lots of wheat kernels for deoxynivalenol and ochratoxin A (case study truck). In Proceedings of the 3rd World Mycotoxin Forum; Noordwijk, the Netherlands.

Biselli, S., Persin, M. & Syben, M. 2008. Investigation of the distribution of deoxynivalenol and ochratoxin A contamination within a 26 t truckload of wheat kernels. Mycotoxin Research 24:2, 98-104.

Chung S, Moon-Chan C, Kyu-Ho L, Yong-Joo K, Soon-Jung H. & Minzan L (2016) Sensing technologies for grain crop yield monitoring systems: A review. J Biosystems Engineering 41:408-417.

De Castro AI, Ehsani R, Ploetz R, Crane, J. H., & Abdulridha, J. (2015a). Optimum spectral and geometric parameters for early detection of laurel wilt disease in avocado. Remote Sensing of Environment 171:33–44. 824

De Castro, A. I., Ehsani, R., Ploetz, R. C., Crane, J. H., & Buchanon, S. (2015b) Detection of laurel wilt disease in avocado using low altitude aerial imaging. PLoS ONE 10(4):e0124642. 827

Del Fiore, A., Reverberi, M., Ricelli, A., Pinzari, F. Serranti, S., Fabbri, A.A., Bonifazi, G., & Fanelli, C. (2010) Early detection of toxigenic fungi on maize by hyperspectral imaging analysis, International Journal of Food Microbiology, 144, 64-71. 830

Di Marco, S., Osti, F., Calzarano, F., Roberti, R., Veronesi, A., & Amalfitano, C. (2011) Effects of grapevine applications of fosetyl-aluminium formulations for downy mildew control on “esca” and associated fungi. Phytopathologia Mediterranea 50(4):S285–S299

EU (2006a) COMMISSION REGULATION (EC) No 401/2006 of 23 February 2006 laying down the methods of sampling and analysis for the official control of the levels of mycotoxins in foodstuffs. https://eur-lex.europa.eu/legal-content/EN/ALL/?uri=CELEX%3A32006R0401

EU (2006b) Commission Regulation (EC) No 1881/2006 of 19 December 2006 setting maximum levels for certain contaminants in foodstuffs

FAO (2017) The Future of Food and Agriculture: Trends and Challenges. Rome. Accessed July 11, 2020. http://www.fao.org/3/a-i6583e.pdf.

FDA (2001) Guidance for Industry: Fumonisin Levels in Human Foods and Animal Feeds.

FDA (2010) Guidance for Industry and FDA: Advisory Levels for Deoxynivalenol (DON) in Finished Wheat Products for Human Consumption and Grains and Grain By-Products used for Animal Feed.

Fischer M. (2002) A new wood-decaying basidiomycete species associated with esca of grapevine: *Fomitiporia mediterranea (Hymenochaetales*). Mycol Prog 1(3):315–324.

Garcia-Cela, E., Kiaitsi, E., Sulyok, M., Medina, A., & Magan, N. (2018). *Fusarium graminearum* in stored wheat: Use of CO_2 production to quantify dry matter losses and relate this to relative risks of zearalenone contamination under interacting environmental conditions. Toxins, 10(2), 86.

Garcia-Cela, E., Kiaitsi, E., Sulyok, M., Krska, R., Medina, A., Petit Damico, I., & Magan, N. (2019). Influence of storage environment on maize grain: CO_2 production, dry matter losses and aflatoxins contamination. Food Additives & Contaminants: Part A, 36(1), 175-185.

Garcia-Cela, E., Sanchez, F. G., Sulyok, M., Verheecke-Vaessen, C., Medina, A., Krska, R., & Magan, N. (2020). Carbon dioxide production as an indicator of *Aspergillus flavus* colonisation and aflatoxins/cyclopiazonic acid contamination in shelled peanuts 863 stored under different interacting abiotic factors. Fungal biology, 124(1), 1-7.

Goovaerts, P., Webster, R., and Dubois, J.P., (1997) Assessing the risk of soil contamination in the Swiss Jura using indicator geostatistics. Environmental and Ecological Statistics, 4, 31–48.

Henry, S. H., F. X. Bosch, T. C. Troxell, and P. M. Bolger. (1999) Reducing liver cancer—global control of aflatoxin. Science 286, 2453–2454.

Hussein, H. S. and Brasel, J. M. (2001) Toxicity, metabolism, and impact of mycotoxins on humans and animals. Toxicology. 167:2, 101-134.

Isakeit, T., Minzenmayer, R. & Sansone, C. (2009) Flutriafol control of cotton root rot caused by *Phymatotrichopsis omnivora*. In: Proceedings of the Beltwide Cotton Conf. 130-133. Cordova, Tenn.: National Cotton Council of America.

Jacquez, G. M., Goovaerts, P., Kaufmann, A., and Rommel, R. (2014) SpaceStat 4.0 User Manual: Software for the space-time analysis of dynamic complex systems (4th ed.). Ann Arbor, MI, BioMedware.

Kerry, R. Ingram, B.R., Goovaerts, P., Meza, F. and Gimenez, D. 2017. 3D LISA: A Flexible Program for Calculating the Local Moran's I in 1, 2 or 3D Illustrated with Examples from Soil Science. GeoComputation 2017, Leeds, September 2017.

Kerry, R. and Oliver, M.A. (2007) Determining the Effect of Skewed Data on the Variogram. I. Underlying Asymmetry. Computers and Geosciences. 33:10, 1212-1232.

Kerry, R. and Oliver, M.A. (2007) Determining the Effect of Skewed Data on the Variogram. II. Outliers. Computers and Geosciences. 33:10, 1233-1260.

Kushiro, M. (2008) Effects of Milling and Cooking Processes on the Deoxynivalenol Content in Wheat. International Journal of Molecular Science. 9, 2127–2145.

Lamb, D. W., (2020) Precision in the Food Chain, Keynote presentation, Virtual International Conference on Precision Agriculture (ICPA) 2020, June 30, 2020.

Maestroni, B. and Cannavan, A. (2011) Sampling strategies to control mycotoxins, Joint FAO/IAEA Division of Nuclear Techniques in Food and Agriculture, International Atomic Energy Agency (IAEA), Austria.

Magan, N., Garcia-Cela, E., Verheecke-Vaessen & Medina, A. (2020). Advances in postharvest detection and control of fungal contamination of cereals. Chapter 14 in Advances in postharvest management of cereals and grains, Edt. Dirk Maier.

Burleigh Dodds Series in Agricultural Science: no. 88, Cambridge, U.K. pp.478. 917 918

Mahlein, A. K., Steiner, U., Hillnhütter, C., Dehne, H. W., & Oerke, E. C. (2012) Hyperspectral imaging for small-scale analysis of symptoms caused by different sugar beet diseases. Plant Methods 8:3.

Mazumder, P. M. and Sasmal, D. (2001) Mycotoxins – Limits and Regulations, Ancient Science of Life, 20, 1-19.

Papadoyannis, I.N., 1990. HPLC in Clinical Chemistry (Chromatographic Science Series), first ed. Marcel Dekker, New York, p. 504.

Paungfoo-Lonhienne, C., Yeoh, Y. K., Kasinadhuni, N. R. P., Lonhienne, T. G., Robinson, N., Hugenholtz, P., Ragan, M. A. & Schmidt, S. (2015). Nitrogen fertilizer dose alters fungal communities in sugarcane soil and rhizosphere. Scientific Reports, 938 5(1), 1-6.

Ranganathan, J., Waite, R., Searchinger, T and Hanson, C. (2018) How to Sustainably Feed 10 Billion People by 2050, in 21 Charts. https://www.wri.org/blog/2018/12/how-sustainably-feed-10-billion-people-2050-21-charts.

Remy, N, Boucher, A. and Wu, J. (2009) Applied Geostatistics with SGeMS: A User's Guide. 1st Edition Cambridge University Press. 284 pp.

Reyns, P., Missotten, B., Ramon, H., & De Baerdemaeker, J. (2002) A review of combine sensors for precision farming. Precision Agriculture 3:169–182

Ribeiro Jr., P.J. and Diggle, P.J. (2001) geoR: A package for geostatistical analysis. R-NEWS, 1: (2), 15-18.

Rivas Casado, M., Parsons, D. J., Weightman, R. N., Magan, N. and Origgi, S. (2009a) Geostatistical analysis of the spatial distribution of mycotoxin concentration in bulk cereals, Food Additives and Contaminants, 26:6, 867-873.

Rivas Casado, M., Parsons, D. J., Magan, N., Weightman, R. M., Battilanic, P. and Pietric, A. (2010) A short geostatistical study of the three-dimensional spatial structure of Fumonisins in stored maize. Mycotoxin Journal, 3 (1): 95-103.

Rivas Casado, M., Parsons, D. J., Weightman, R. M., Magan, N. & Origgi, S. (2009b) Modelling a two-dimensional spatial distribution of mycotoxin concentration in bulk commodities to design effective and efficient sample selection strategies, Food Additives and Contaminants, 26:9, 1298-1305.

Searchinger, T., Waite, R., Hanson, C., Ranganathan, J. and Matthews, E. (2019) Creating a Sustainable Food Future: A Menu of Solutions to Feed Nearly 10 Billion People by 2050 (Final Report).

Semple, R.L., Frio, A.S., Hicks, P.A. and Lozare, J.V. (Eds.) (1989) Mycotoxin Prevention and Control in Foodgrains, FAO, Bankok, Thailand. http://www.fao.org/3/x5036e/x5036E00.htm#Contents accessed July 2020.

Van Meirvenne, M. and Goovaerts, P., 2001. Evaluating the probability of exceeding a site-specific soil cadmium contamination threshold. *Geoderma*, 102, 75–100.

Wang, Y., Wang, L., Liu, F., Wang, Q., Selvaraj, J. N., Xing, F., Zhao, Y., and Liu, Y. (2016). Ochratoxin A Producing Fungi, Biosynthetic Pathway and Regulatory Mechanisms. *Toxins*, *8*(3), 83.

Webster, R. and Oliver, M. A. (1992) Sample adequately to estimate variograms of soil properties, Journal of Soil Science, 43, 177-192.

Table 1. Univariate and bi-variate global Moran's I values and variogram and cross-variogram parameters for DON and OTA contamination in the truck load of grain

Variable(s)	Global Moran's I	*p* value	Model	Nugget:sill ratio (%)	Variogram range (m)
DON	0.468	0.001	Spherical	13	4.00
OTA	-0.012	0.494	Spherical	62	3.57
OTA NST	0.124	0.001	Spherical	30	1.00
DON and OTA NST	0.157	0.001	Gaussian	0	3.00

Table 2. Univariate and bivariate global Moran's I for NS FB_1 and FB_2 within and between layers and parameters of 2D and 3D variograms for single layers and the whole grain pile .

Variable(s)	Global Moran's I	*p* value	Model	Nugget:sill ratio (%)	Variogram range (m)
FB_1 (layer 1)	0.029	0.158	*Gaussian*	*50*	*3.86*
FB_1 (layer 2)	-0.021	0.500	*Spherical*	*67*	*2.78*
FB_1 (layer 3)	0.047	0.054	Spherical	52	1.02
FB_2 (layer 1)	-0.060	0.170	*Spherical*	*67*	*1.98*
FB_2 (layer 2)	-0.009	0.400	---	---	---
FB_2 (layer 3)	0.019	0.164	Spherical	48	0.98
FB_1 layers 1 and 2	0.069	0.115	---	---	---
FB_1 layers 2 and 3	**0.119**	**0.003**	---	---	---
FB_1 layers 1 and 3	0.022	0.326	---	---	---
FB_2 layers 1 and 2	0.035	0.204	---	---	---
FB_2 layers 2 and 3	**0.111**	**0.016**	---	---	---
FB_2 layers 1 and 3	-0.003	0.499	---	---	---
FB_1 all layers (3D)	0.048	---	Exponential	50	4.00
FB_2 all layers (3D)	0.068	---	Exponential	48	3.00

Bold values are significant at p=0.05, *Italics* show REML variogram parameters, --- missing/not valid

Table 3. Percentages of points in the sample data points exceeding EU and FDA toxin limits

Toxin	EU limit (ppb)	FDA limit (ppb)	Mean batch concentration (ppb)	% of batch above EU limit	% of Batch above FDA limit
DON	1250	1000	1342	55 %	88 %
OTA	5	No limit	0.57	1 %	---
FB_1+FB_2	1000, 4000	4000	2495+1225=3720	83 %, 38%	38 %

Table 4. Percentages of points in the kriged data exceeding EU and FDA toxin limits

Toxin	EU limit (ppb)	FDA limit (ppb)	Mean batch concentration (ppb)	% of batch above EU limit	% of Batch above FDA limit
DON	1250	1000	1354	53 %	99%
OTA	5	No limit	2.68	0.1 %	---
FB_1+FB_2	1000, 4000	4000	2061+943=3004	99 %, 16%	16 %

Table 5. Summary Statistics of Percentage of Kriged Points above the Mean Concentrations (assumed equal to legislative limit) for 100 Simulated Realizations

Toxin	Mean % above mean concentration	Range of % above mean concentration	Interquartile range of % above mean concentration
DON	53	9-88	37-73
OTA	26	13-36	22-29
FB_1	43	38-48	42-44
FB_2	51	27-72	44-57

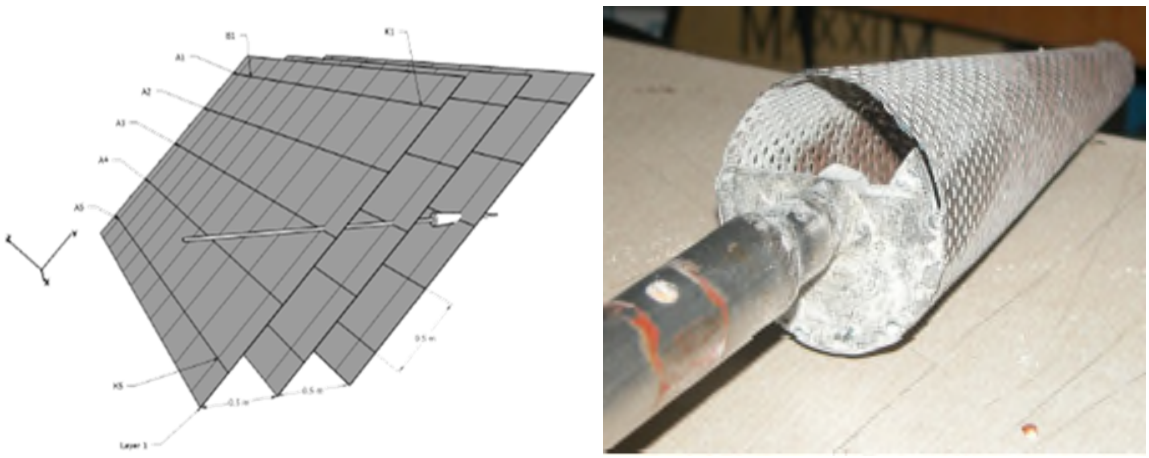

Figure 1. (a) Sampling scheme and (b) sampling probe (Rivas Casado et al., 2010).

(a) DON (skew=1.21)	**(b) OTA (skew=4.36)**
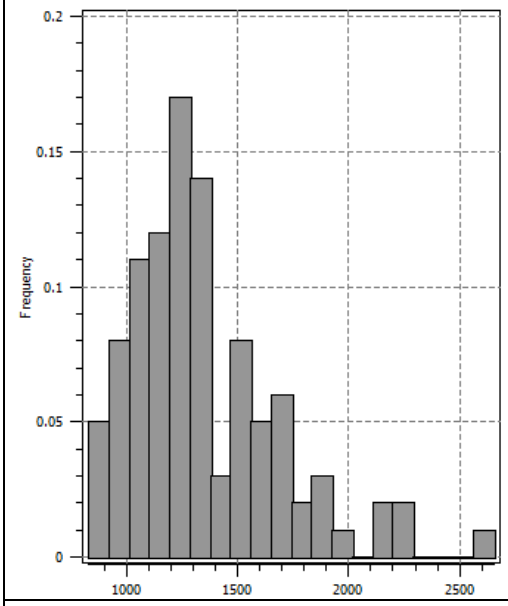	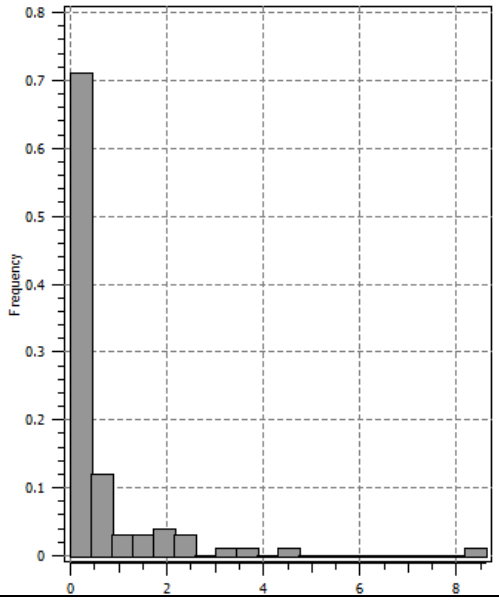
(c) DON variogram	(d) OTA variogram
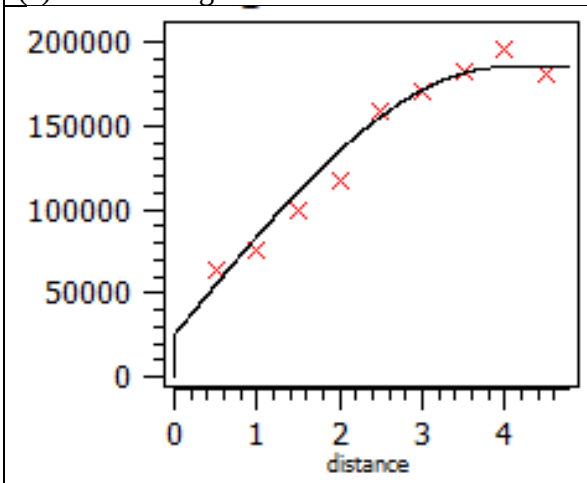	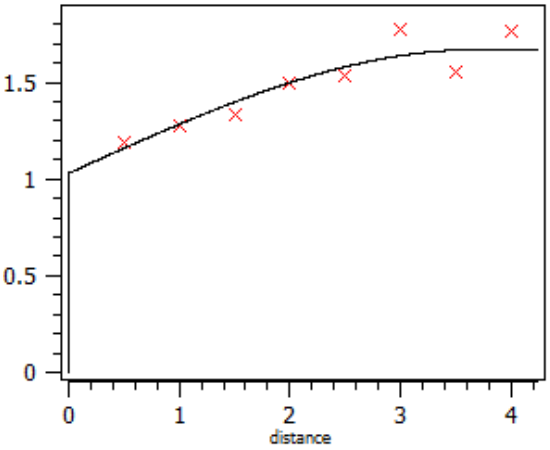
(e) OTA NS variogram	(f) DON and OTA NS cross variogram

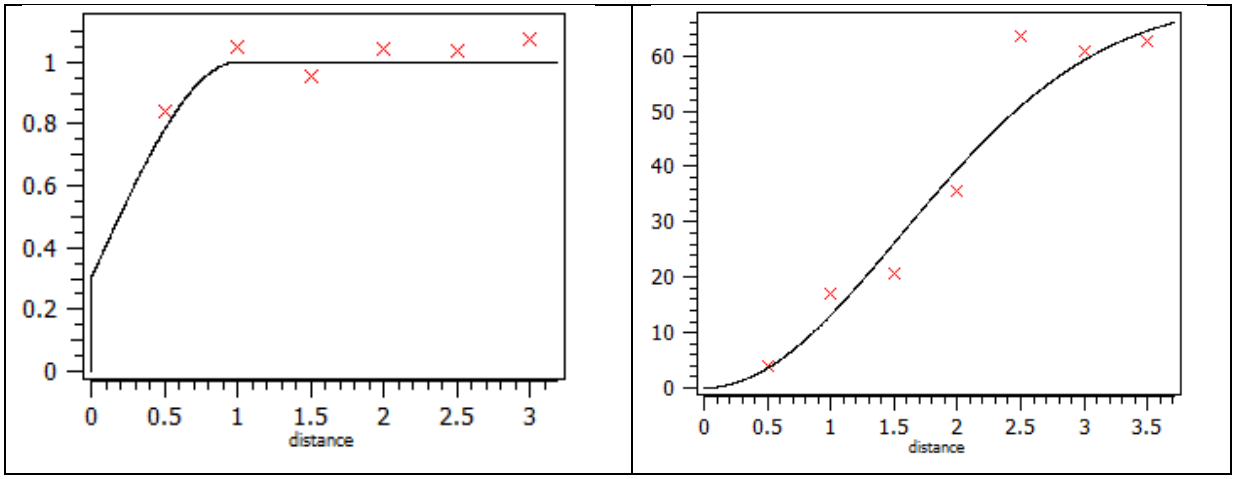

Figure 2. Histograms of Mycotoxins in ppb in the truck load of grain (a) DON and (b) OTA and 2D variograms of (c) DON, (d) OTA, (e) OTA NS and (f) cross variogram for DON and OTA NS

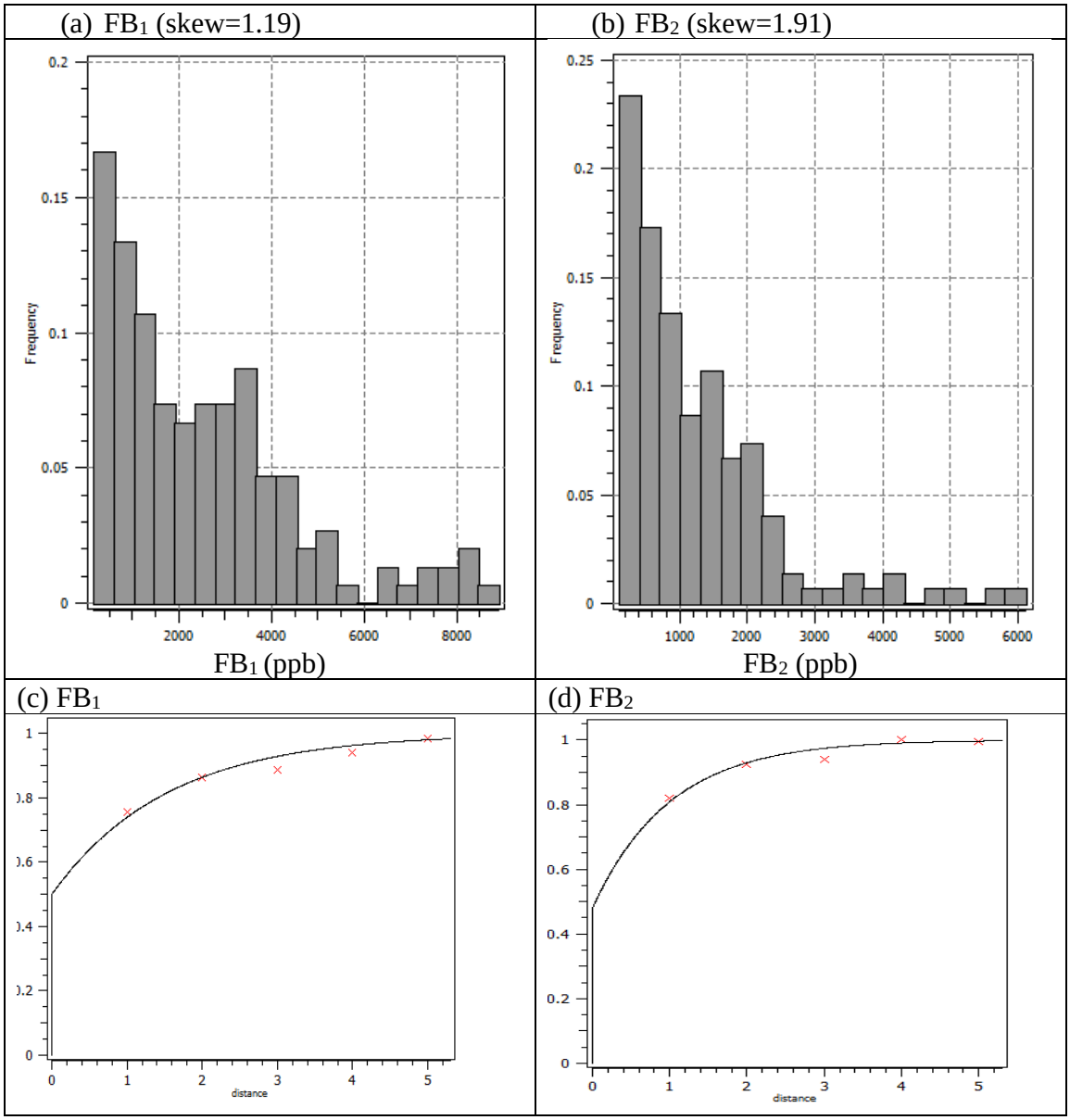

Figure 3. Histograms of Mycotoxin concentrations in (ppb) (a) FB_1 and (b) FB_2 and variograms for (c) FB_1 and (d) FB_2 in the grain pile

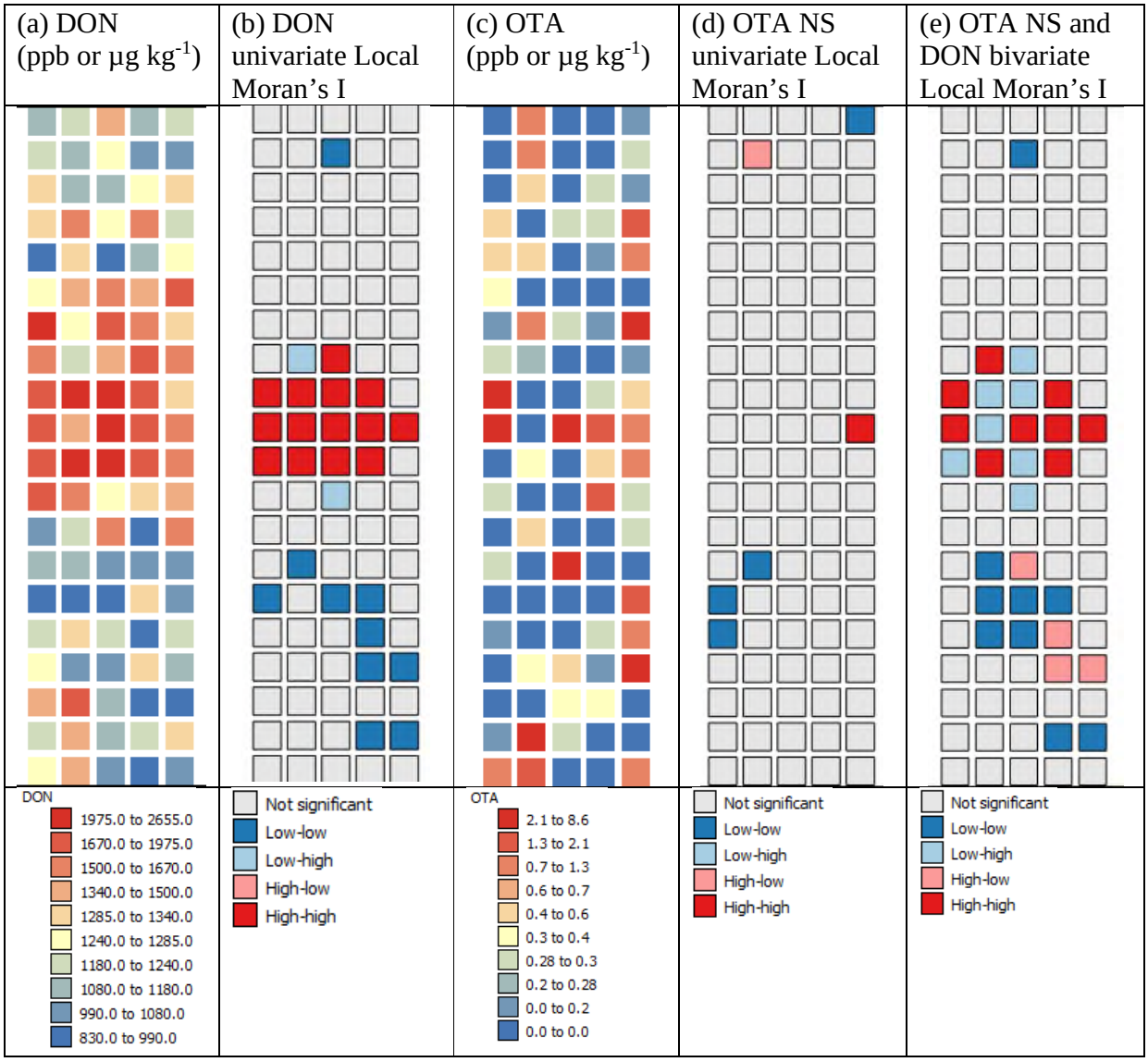

Figure 4. Maps of raw values of DON (a) and OTA (c) and distribution and clusters from uni- (b, d) and bi-variate (e) LMI analysis of the mycotoxin concentrations in the truck load of grain

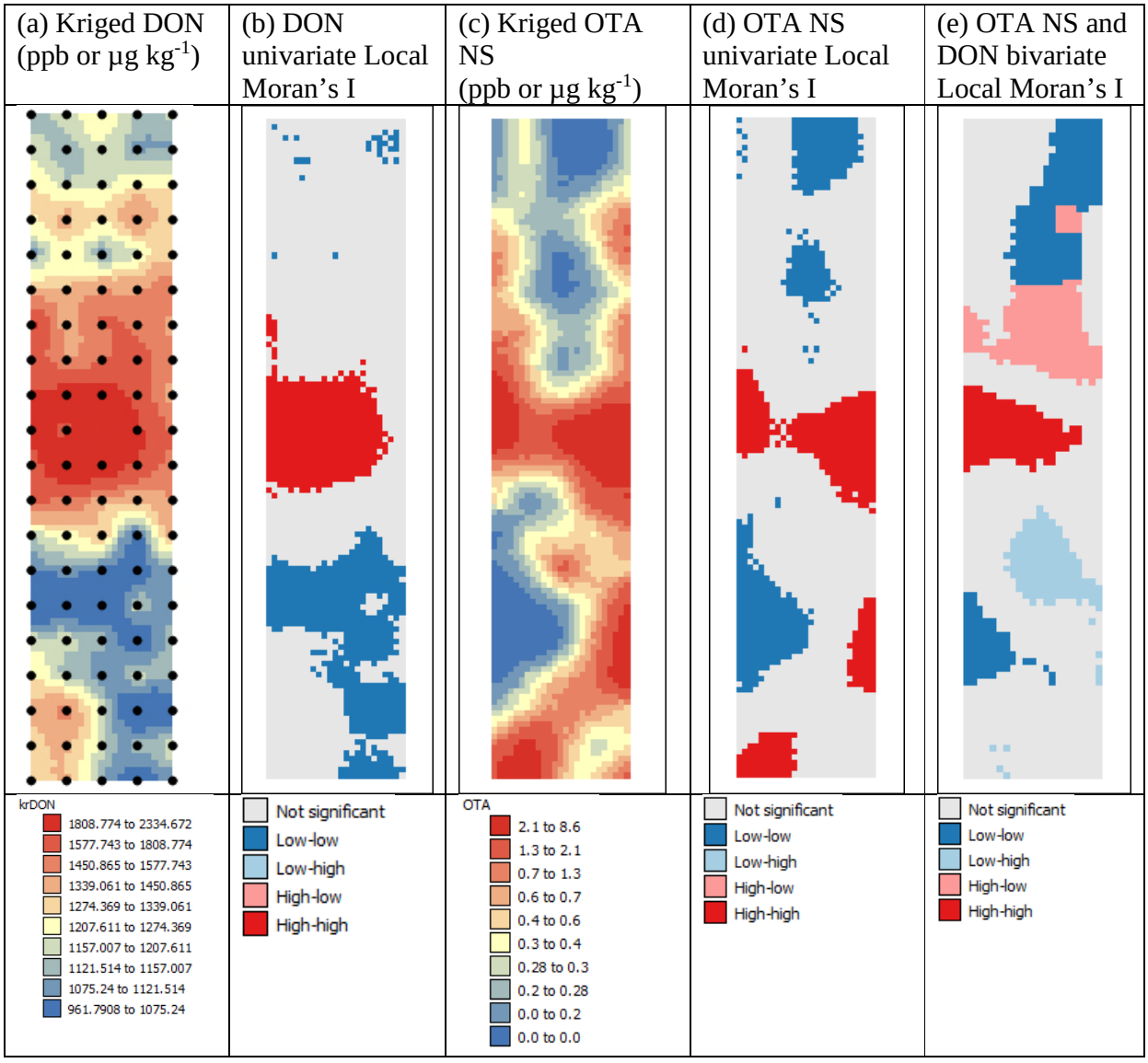

Figure 5. Kriged maps of DON (a) and OTA (c) distribution and clusters from uni- (b, d) and bi-variate (e) LMI analysis of the mycotoxin concentrations in the truck load of grain

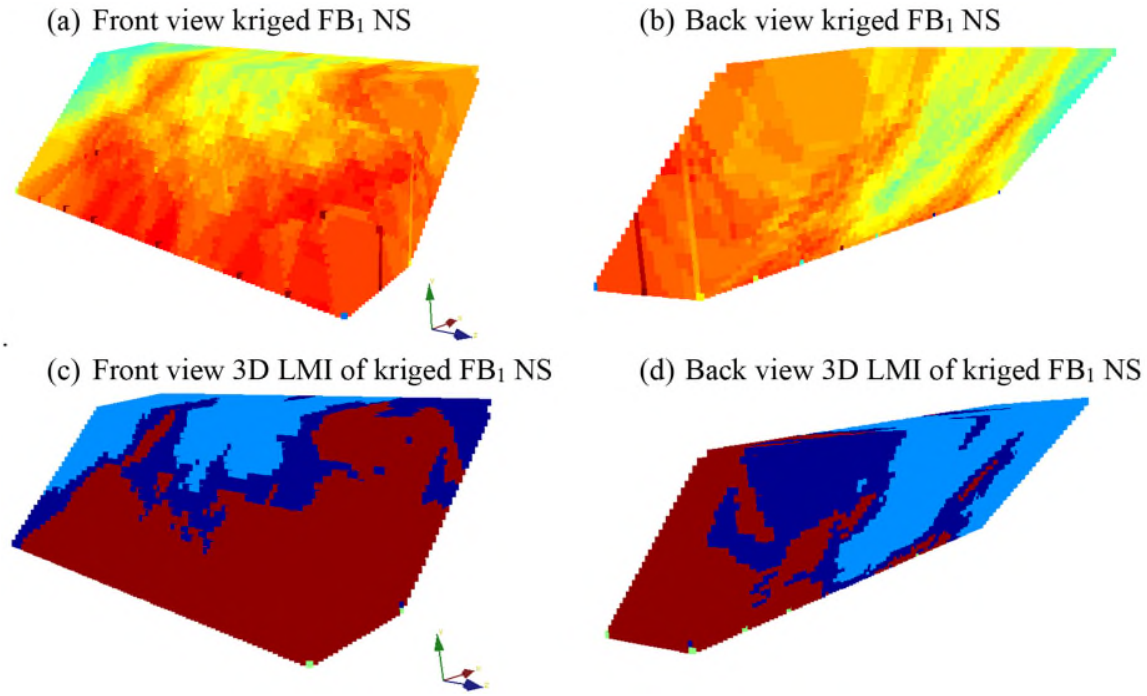

Figure 6. Front and back views of Kriged FB_1 NS concentrations (low values yellow, green and blue and high values orange and red) and LMI for the grain pile (p=0.05 HH cluster (red), LL cluster (pale blue), NS values (dark blue)).